

# Burning Velocities of Mixtures of Air with Methanol, Isooctane, and Indolene at High Pressure and Temperature

MOHAMAD METGHALCHI

*Northeastern University, Boston, Massachusetts*

and

JAMES C. KECK

*Massachusetts Institute of Technology, Cambridge, Massachusetts*

Burning velocities of mixtures of air with methanol, isooctane, and indolene (RMFD303) have been measured using the constant volume bomb method for fuel-air equivalence ratios  $\phi = 0.8-1.5$  over the pressure and temperature ranges  $p = 0.4-50$  atm and  $T = 298-700$ K. The effect of adding simulated combustion products to stoichiometric isooctane-air mixtures was also studied for diluent mass fractions  $f = 0-0.2$ . Over the range studied, the results can be fit within  $\pm 10\%$  by the functional form  $S_u = S_{u0} (T_u/T_0)^\alpha (p/p_0)^\beta (1-2.1f)$ , where  $S_{u0}$  depends on fuel type and equivalence ratio and  $\alpha$  and  $\beta$  depend only on equivalence ratio. In overlapping ranges, the results agree well with those previously reported.

## 1. INTRODUCTION

The laminar burning velocity is among the most fundamental properties characterizing the combustion of homogeneous fuel-air mixtures. It is also an important parameter entering several current models of turbulent combustion [1-3] and wall quenching [4, 5].

Although encouraging progress is being made in the development of basic chemical kinetic models for predicting laminar burning velocities [6, 7], such models are extremely complex and require experimental verification. By contrast, the direct measurement of laminar burning velocities is relatively easy and accurate and the results can be used both for direct practical applications to internal combustion engines and burners and for critical testing of basic theoretical models.

Numerous measurements of the burning velocities as a function of temperature at atmospheric

pressure have been made using tubes and burners for a wide variety of fuels [8, 9]. Measurements for a more limited range of fuels have also been made at high pressures and temperatures using constant volume bombs. The fuels studied by this method include methane [10, 15], propane [10, 15, 16], butane [17], 2-methylpentane [12], *n*-heptane [10, 18], isooctane [10, 18], acetylene [15, 19], ethylene [12, 15], benzene [18], toluene [12], and methanol [10].

The present study is an extension of the work on propane reported in Ref. [16] and includes the pure fuels methanol and isooctane and the blended fuel indolene (RMFD303). The measurements were carried out in a heated spherical combustion bomb and the emphasis was on the high-temperature and pressure region important for applications to internal combustion engines and gas turbine burners. The experimental apparatus and procedure are reviewed in the next section. A rela-

tively simple but accurate method for determining the laminar burning velocities from the pressure records is described in Section 3. The method includes explicit consideration of corrections to bomb measurements necessary to account for (1) wall heat losses, (2) the thermal preheat zone ahead of the reaction front, (3) energy input by the spark, (4) heat losses to the ignition electrodes, (5) radiation from the burned gas, and (6) the temperature gradient in the burned gas. The results are presented in Section 4 and a discussion and comparison with previous work is given in Section 5. A summary is given in the last section. Expressions for estimating the corrections listed above are given in the appendix.

## 2. EXPERIMENTAL APPARATUS AND PROCEDURES

A detailed description of the experimental apparatus used for the present study is given in Ref. [16]. Only its general features and the procedures used to make measurements will be reviewed here.

The combustion bomb had an inside diameter of 15.24 cm and was designed for pressures up to 700 atm. It was located in a glass-wool oven and could be heated electrically to a temperature of 500K. Two 1.5-mm diam extended stainless steel electrodes tapered to a point at their tips were used to form the spark gap at the center of the bomb.

Permanent gas pressures were measured by Bourdon gauges calibrated against a dead weight tester. Fuel pressures were measured by a mercury manometer which could be heated up to 400K to avoid condensation of low vapor pressure components of blended fuels.

The dynamic pressure rise inside the bomb during combustion was measured with a Kistler Model 603B1 piezoelectric pressure transducer coated with Dow Corning high-vacuum grease to reduce its thermal sensitivity. The pressure transducer was assumed to be linear and a calibration point at high pressure was obtained during each run using a balanced pressure indicator. Spherical symmetry and centering of the flame front were checked by three ionization probes which measured the arrival time of the flame at the wall. An internal consist-

ency check on the models used for calculating the burning velocities was obtained using a laser shadowgraph system which measured the arrival time of the flame front at a known radius.

For the pure fuels methanol and isooctane, the fuel-air mixtures could be prepared using either the method of partial pressures or by using a calibrated syringe to inject the desired quantity of liquid fuel into the bomb through a silicone septum. For the multicomponent fuel RMFD303, it was necessary to use the injection system to avoid altering the fuel composition.

To make a measurement, the bomb was first heated to the desired temperature as determined by four thermocouples at various locations. The fuel was then introduced and 5 min were allowed for the system to come to thermal equilibrium at the desired pressure. The fuel pressure manometer was then sealed off and air and diluent gases were introduced to produce the desired mixture.

Again, 5 min were allowed for motions to damp out and the system to come to thermal equilibrium.

After the filling procedure was completed, the pressure transducer was zeroed and the mixture ignited. The analog signals from the pressure transducer and the laser were fed directly to a microcomputer and the digitized data were transferred automatically from the microcomputer to the host computer for analysis. The ionization probe signals used to determine arrival times at the wall were recorded separately by digital clocks and fed to the host computer by the operator.

## 3. THEORETICAL MODEL

To determine the laminar burning velocity from the measured pressure rise in the combustion bomb, it is first necessary to calculate the burned gas mass. In Ref. [16], this was done by a simultaneous numerical solution of the conservation equations for energy and volume under the assumption that heat losses were negligible. In the present work, the analysis has been simplified and extended to include explicit consideration of the corrections for several potentially important heat transfer processes.

### 3.1. Thermodynamics of Combustion

The thermodynamic model employed to analyze the combustion process in the bomb is based on the following assumptions:

1. The unburned gas is initially at rest and has uniform temperature and composition.
2. The thickness of the reaction zone is negligible and the gas within the bomb consists of a burned fraction  $x$  at local thermodynamic and chemical equilibrium and an unburned fraction  $1-x$  at local thermodynamic equilibrium but with fixed chemical composition.
3. The pressure is independent of position and a function of time only.
4. The reaction front is smooth and spherical.

Under these conditions the equation for the specific volume of the gas in the bomb can be written

$$v_1 = \int_0^x v_b(x', x) dx' + \int_x^1 v_u(x', x) dx' \quad (1)$$

where  $v$  denotes specific volume and the subscripts 1, b, and u denote initial conditions, burned gas and unburned gas, respectively. Introducing the adiabatic burned and unburned specific volumes  $v_b^0$  and  $v_u^0$ , Eq. (1) can also be written

$$(1 + a_b + a_u)v_1 = \int_0^x v_b^0(x', x) dx' + (1-x)v_u^0(x), \quad (2)$$

where

$$a_b = \int_0^x (v_b^0 - v_b) dx/v_1 \quad (3)$$

and

$$a_u = \int_x^1 (v_u^0 - v_u) du/v_1 \quad (4)$$

are fractional displacement volumes for burned and unburned gas, respectively. The major contributions to  $a_u$  come from the thermal boundary layer on the bomb wall and the thin preheat layer in the

unburned gas ahead of the reaction zone, while the major contributions to  $a_b$  come from the energy input by the spark, the thermal boundary layer on the ignition electrodes, radiation heat loss from the hot burned gas, and conduction heat loss due to the radial temperature gradient in the burned gas.

Differentiating Eq. (2) with respect to  $p$  and using the ideal gas equation of state

$$pv = RT, \quad (5)$$

where  $p$  is the pressure,  $T$  is the temperature, and  $R$  is the specific gas constant, we obtain

$$p(v_f^0 - v_u^0) \frac{dx}{dp} = \eta_f^0 \int_0^x v_b^0 dx' + (1-x)\eta_u^0 v_u^0 + v_1 \left( p \frac{d}{dp} (a_b + a_u) + \eta_f^0 a_\eta \right), \quad (6)$$

where

$$\eta = - \left( \frac{\partial \ln v}{\partial \ln p} \right)_s = \frac{1}{\gamma} \left( 1 - \frac{p}{R} \left( \frac{\partial R}{\partial p} \right) \right)_T \quad (7)$$

is a slowly varying function of temperature and pressure,

$$\gamma = c_p/c_v = 1 + R/c_v \quad (8)$$

is the ratio of the constant pressure specific heat  $c_p$  to the constant volume specific heat  $c_v$ ,

$$a_\eta = \int_0^x \left( \frac{\eta_b^0}{\eta_f^0} - 1 \right) \frac{v_b^0}{v_1} dx' \quad (9)$$

is a correction for the variation of  $\eta$  in the burned gas which vanishes if  $R_b$  and  $c_{vb}$  are constant, the subscript f denotes burned gas conditions immediately behind the reaction front, and the subscripts s and T denote processes at constant entropy and temperature, respectively.

Combining Eqs. (2) and (6) and using Eq. (5), we find

$$\begin{aligned} \frac{dx}{dp} = & \frac{\eta_f^0 v_1}{R_f^0 T_f^0 - R_u T_u^0} \left( 1 - (1-x) \right. \\ & \times \left( 1 - \frac{\eta_u^0}{\eta_f^0} \right) \frac{v_u^0}{v_1} + a_\eta + a_b + a_u \\ & \left. + \frac{p}{\eta_f^0} \left( \frac{da_b}{dp} + \frac{da_u}{dp} \right) \right), \end{aligned} \quad (10)$$

where  $T_f^0$  is the adiabatic flame temperature corresponding to the unburned gas temperature  $T_u^0$ .

Under the conditions of the present measurements,  $(1 - \eta_u^0/\eta_f^0) \approx (1 - \gamma_f^0/\gamma_u^0) \sim 0.1$  and Eq. (10) can be solved easily by iteration.

Assuming as a first approximation that  $R$  and  $\gamma$  are constant, so that  $a_\eta = 0$  and  $\eta = 1/\gamma$ , we find for isenthalpic combustion

$$\begin{aligned} \frac{d}{dp} (R_f^0 T_f^0 - R_u T_u^0) \\ = \left( R_f^0 \frac{c_{p_u}^0}{c_{p_f}^0} - R_u \right) \frac{dT_u^0}{dp} \\ = \left( \frac{1}{\gamma_u^0} - \frac{1}{\gamma_f^0} \right) v_u^0. \end{aligned} \quad (11)$$

By using this relation and, further, assuming that  $a_b = a_u = 0$ , Eq. (10) can be integrated to give

$$\begin{aligned} x \approx & \frac{p_1 v_1}{\gamma_f^0 (R_f^0 T_f^0 - R_u T_u^0)} \\ & \times \left( \frac{p}{p_1} - 1 - \left( \frac{\gamma_u^0 - \gamma_f^0}{\gamma_u^0 - 1} \right) \right) \\ & \times \left( \left( \frac{p}{p_1} \right)^{(\gamma_u^0 - 1)/\gamma_u^0} - 1 \right). \end{aligned} \quad (12)$$

This expression can now be substituted back into the right side of Eq. (10) to obtain an accurate value for  $dx/dp$  including the correction terms  $a_u$ ,  $a_b$ , and  $a_\eta$ . It can also be substituted into Eq. (2)

to obtain the burned gas volume fraction

$$\begin{aligned} V_f/V_c = & \int_0^x (v_b/v_1) dx' \\ = & 1 + a_u - (1-x)(v_u^0/v_1), \end{aligned} \quad (13)$$

where  $V_c$  is the combustion bomb volume.

### 3.2. Laminar Burning Velocity

Using Eqs. (10), (12), and (13) and the measured dynamic pressure, the laminar burning velocity can be calculated from the definition

$$\begin{aligned} S_u = & \frac{m_1}{\rho_u A_f} \frac{dx}{dt} \\ = & \frac{\rho_1}{\rho_u^0} \left( \frac{V_c}{V_f} \right)^{2/3} \frac{r_c}{3} \left( \frac{dx}{dp} \right) \frac{dp}{dt}, \end{aligned} \quad (14)$$

where  $m_1 = \rho_1 V_c$  is the mass of gas in the bomb,  $\rho = 1/v$  is the gas density,  $A_f$  is the area of the reaction front,  $r_c$  is the radius of the combustion bomb, and we have assumed the reaction front is spherical.

In the evaluation of Eq. (14), the burned gas properties were computed using an approximation to equilibrium properties developed by Martin and Heywood [20], and the unburned gas properties were computed using thermodynamic data from JANAF tables [21] and Rossini et al. [22] for the individual species in the mixture and the assumption of fixed composition.

The correction  $a_\eta$  for variable burned gas properties was calculated using Eq. (9) and was found to be of order 0.01  $x$ . The corrections  $a_u$  and  $a_b$  for heat transfer and temperature gradients in the preheat layer and burned gas were calculated using the relations given in the appendix. In no case did these corrections exceed 1%, and in most cases they were substantially less.

Other possible sources of error which were considered but found to be negligible were (1) buoyant rise of the fire ball, (2) charge stratification of the mixture, and (3) wrinkling of the flame front.

Buoyant rise and spherical symmetry of the reaction front were monitored by the wall ionization

probes, and no significant rise or departure from spherical symmetry was observed under any of the conditions studied. However, even if some rise or distortion occurs, the results will not be affected as long as the surface-to-volume ratio remains approximately constant.

Charge stratification is governed by the relation

$$\rho_{ah}/\rho_{al} = \exp(-2r_{cg}/R_a T_1),$$

where  $\rho_{ah}$  and  $\rho_{al}$  are the densities of species  $a$  at the top and bottom of the bomb and  $g = 9.8 \text{ m/s}^2$  is the gravitational acceleration. The maximum variation in the fuel-air ratio calculated from this equation for the case of isooctane-air mixtures was  $\sim 0.01\%$ , which is completely negligible.

Wrinkling of the flame front will alter the calculated burning velocity primarily through its effect on the area of the flame front. Babkin et al. [18] and Groff [23] have observed cellular flame structure in constant volume bombs similar to that used in the present study. On the basis of these observations it does not appear that wrinkling could increase the flame area or decrease the burning velocity by more than a few percent at any of the conditions studied. This is an effect worthy of further investigation, however.

The most important measurement errors were those arising from the absolute calibration of the Kistler pressure transducer and the 12-bit precision of the A/D converter. Both these errors were estimated to be  $\pm 2\%$ , which leads to an estimated error of  $\pm 3\%$  in the value of the burning velocity. This is consistent with observed point-to-point and run-to-run variations in the measurements.

## 4. RESULTS

Measurements of the burning velocities of mixtures of air with methanol, isooctane, and RMFD303 were made as a function of equivalence ratio, temperature, and pressure. The properties of the latter fuel are given in Table 1. In addition, the effect of adding simulated combustion products to stoichiometric isooctane-air mixtures was investigated.

### 4.1. Temperature and Pressure Dependence

Measurements of the burning velocities for the three fuel-air mixtures studied are shown in Figs.

TABLE 1  
Physical Properties and Chemical Analysis of  
RMFD-303 (Indolene)

Stoichiometric fuel-air ratio	0.06988
Lower heat of combustion (K cal/gm)	10.15
Motor octane rating	88.3
Research octane rating	101.4
Specific gravity	0.765
Average molecular formula	$C_{7.8}H_{13.214}$
Component weight percents	
Aromatic	45.3%
Olefin	13.9%
Parafin	40.8%
Component molecular percents	
Aromatic	52.49%
Olefin	9.36%
Parafin	38.16%
Component typical hydrocarbon	
Aromatic	Toulene
Olefin	Undecene
Parafin	Isooctane

1-3 as a function of the unburned gas temperature for fuel-air equivalence ratios  $\phi = 0.8, 1.0,$  and  $1.2$ . The three sets of points at each equivalence ratio show the burning velocities along unburned gas isentropes starting at the initial temperature  $T_i$  specified and the initial pressures  $p_i = 0.4, 1.0,$  and  $2.0 \text{ atm}$ . In general each isentrope includes overlapping points from three runs, the first starting at the specified  $T_i$  and the remaining two at  $T_1 = 400$  and  $500\text{K}$ . In some cases it was not possible to obtain data at all three conditions. For methanol at  $p_i = 2.0 \text{ atm}$ , the vapor pressure was too low to permit runs at  $T_1 = 298\text{K}$  and problems with vapor pressure measurement prevented runs at  $T_1 = 500\text{K}$ . For isooctane at  $p_i = 0.4 \text{ atm}$  the mixture could not be ignited at  $T_1 = 298\text{K}$  and autoignition occurred at  $T_1 = 500\text{K}$  for all isentropes.

For any single run, the temperature range spanned was about a factor of 1.5. Thus there is considerable overlap in points for successive runs on the same isentrope. In general, agreement in the overlapping regions was within  $\pm 3\%$  and no systematic trends were observed. This provided a valuable internal consistency check on measurements as well as supporting the assumptions of

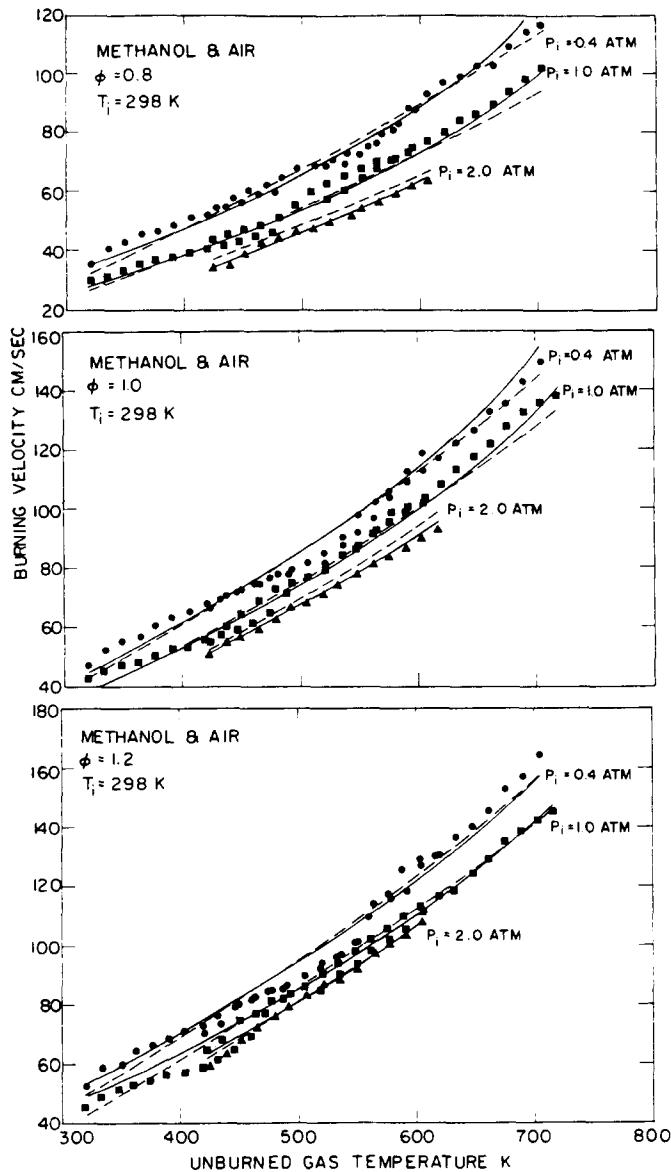


Fig. 1. Burning velocity of methanol-air mixtures for fuel-air equivalence ratios  $\phi = 0.8, 1.0,$  and  $1.2$ . Points show measured velocities along unburned gas isentropes starting at values of  $T_i$  and  $p_i$  indicated. Dashed and solid curves show least squares fits of Eqs. (15) and (19) to points.

negligible reaction front thickness and negligible preflame reactions.

The measured burning velocities in Figs. 1-3 have been fit by two functional forms. The first is the simple power law

$$S_u = S_{u0}(T_u^0/T_0)^\alpha (p/p_0)^\beta, \quad (15)$$

where  $T_0 = 298\text{K}$  and  $p_0 = 1 \text{ atm}$  are the reference temperature and pressure and  $S_{u0}$ ,  $\alpha$  and  $\beta$  are constants for a given fuel, equivalence ratio, and diluent gas fraction. The values of  $S_{u0}$  and  $\alpha$  and  $\beta$  for the three fuel-air mixtures studied are shown in Table 2 and Fig. 4 as a function of equivalence ratio for zero diluent fraction. Also

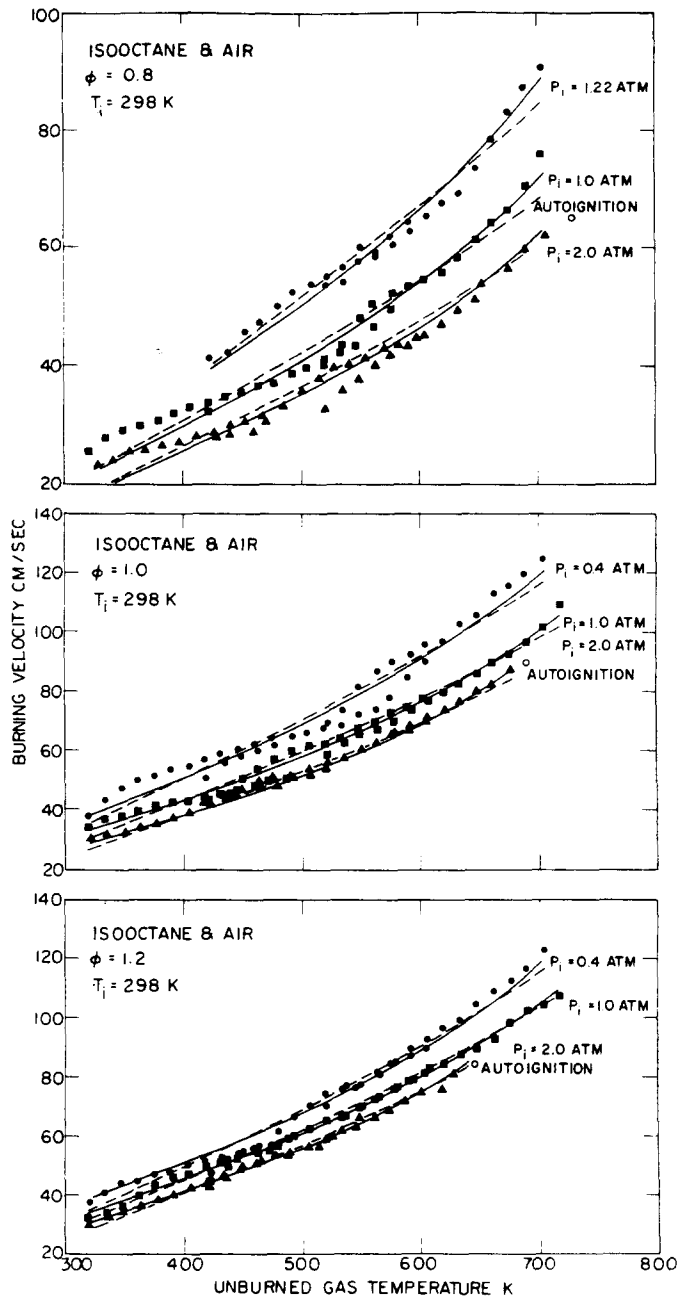


Fig. 2. Burning velocity of isooctane-air mixtures for fuel-air equivalence ratios  $\phi = 0.8, 1.0,$  and  $1.2$ . Points show measured velocities along unburned gas isentropes starting at values of  $T_i$  and  $p_i$  indicated. Dashed and solid curves show least squares fits of Eqs. (15) and (19) to points.

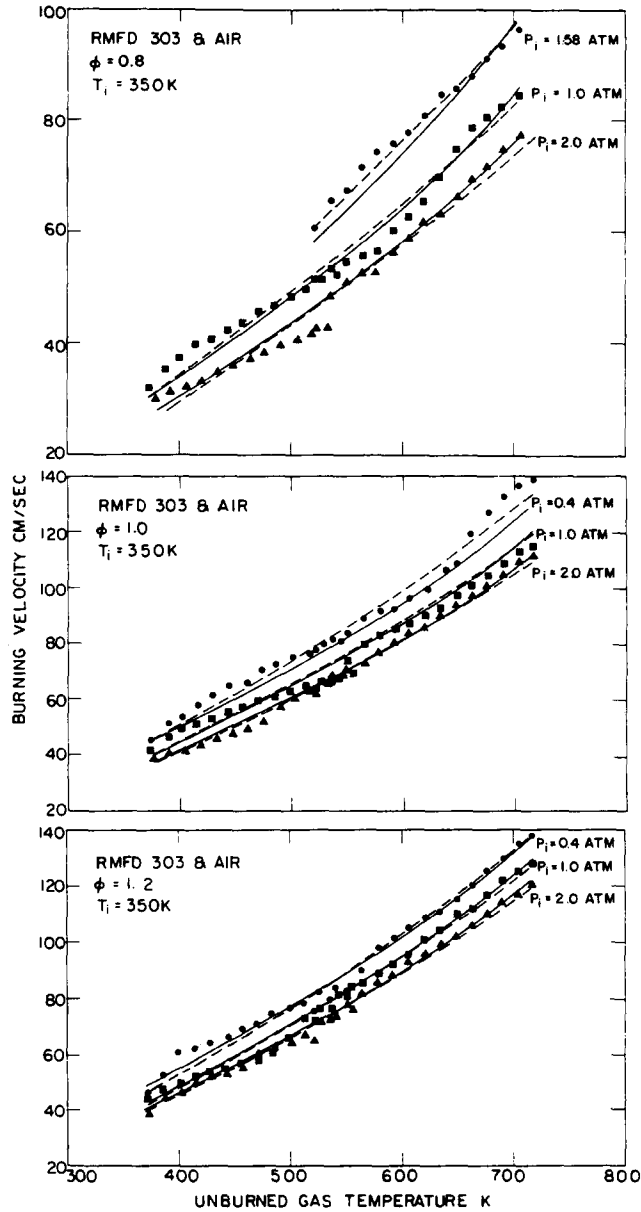


Fig. 3. Burning velocity of RMFD303-air mixtures at fuel-air equivalence ratios  $\phi = 0.8, 1.0,$  and  $1.2$ . Points show measured velocities along unburned gas isentropes starting at values of  $T_1$  and  $p_1$  indicated. Dashed and solid curves show least squares fits of Eqs. (15) and (19) to points.

shown are the corresponding values for propane obtained from Ref. [16] and the standard deviations of an individual point from the power law fit. The results are shown by the dashed curves in Figs. 1-3. It can be seen that the overall fit is

quite good, although there appear to be some small systematic deviations of the points from the curves particularly at temperatures less than 400K, where the fitted curves are too low. It can also be seen from Table 2 and Fig. 4 that the temperature

**TABLE 2**  
Parameters  $S_{u0}$ ,  $\alpha$ , and  $\beta^a$

Fuel	$\phi = 0.8$	$\phi = 1.0$	$\phi = 1.2$
$S_{u0}$ (cm/s)			
Methanol	23.58	32.69	38.11
Propane	23.20	31.90	33.80
Isooctane	19.25	27.00	27.63
RMFD-303	19.15	25.21	28.14
$\alpha$			
Methanol	2.47	2.11	1.98
Propane	2.27	2.13	2.06
Isooctane	2.36	2.26	2.03
RMFD-303	2.27	2.19	2.02
$\beta$			
Methanol	-0.21	-0.13	-0.11
Propane	-0.23	-0.17	-0.17
Isooctane	-0.22	-0.18	-0.11
RMFD-303	-0.17	-0.13	-0.087
$\Delta$ (cm/s)			
Methanol	3.15	3.93	3.55
Propane	2.94	3.03	2.75
Isooctane	2.47	3.74	2.55
RMFD-303	2.12	3.52	2.83

<sup>a</sup> Obtained by fitting the power law relation

$$S_u = S_{u0}(T_u^0(K)/298)^\alpha(p(\text{atm}))^\beta$$

to the points in Figs. 1-3.  $\Delta$  is the standard deviation of a point from the fitted curve.

and pressure exponents  $\alpha$  and  $\beta$  are independent of fuel types within the estimated experimental error and can be represented by the expression

$$\alpha = 2.18 - 0.8(\phi - 1) \tag{16}$$

and

$$\beta = -0.16 + 0.22(\phi - 1) \tag{17}$$

The reference velocities  $S_{u0}$  are a weak function of fuel type and can be fit by a second-order polynomial of the form

$$S_{u0} = B_m + B_2(\phi - \phi_m)^2, \tag{18}$$

where the parameters  $B_m$  and  $B_2$  are given in Table 3A and we have set  $\phi_m$  equal to the value given for the corresponding fuel in Table 3B.

The second relation used to correlate the data in Figs. 1-3 is the Arrhenius form

$$S_u = U(T_u^0/T_0)(p/p_0)^b \exp(-E_A/2R_f T_f^0) \tag{19}$$

employed by Lavoie [24] to correlate the data from a number of previous velocity measurements. This relation is based on the thermal theory of laminar flame propagation developed by Zeldovich and Frank-Kamenetsky and presented by Semenov [25]. The best fit parameters  $U$ ,  $b$ , and  $E_A$  for this form are shown in Table 4, and

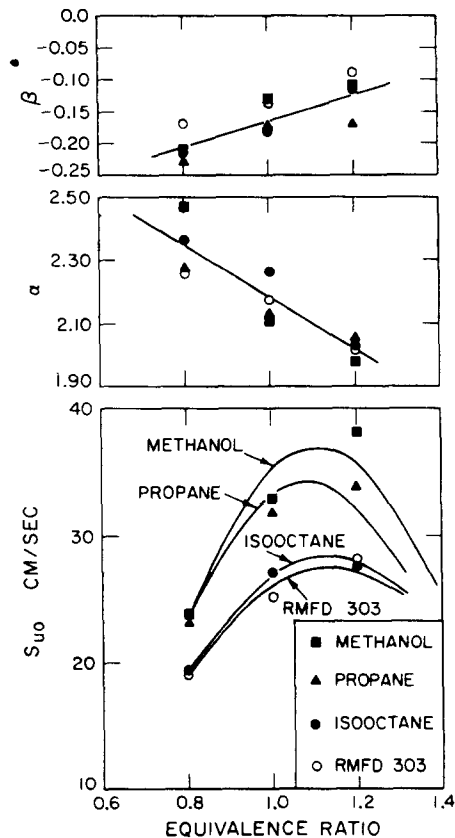


Fig. 4. Parameters  $S_{u0}$ ,  $\alpha$ , and  $\beta$  for methanol, isooctane, and RMFD303 obtained from least squares fit of Eq. (15) to points in Figs. 1-3. Also shown are data for propane obtained from Ref. [16]. The curves show least squares fits of Eqs. (16)-(18) to the points.

TABLE 3A  
Parameters  $B_m$  and  $B_2^a$

	$\phi_m$	$B_m$ (cm/s)	$B_2$ (cm/s)	$\Delta$ (m/s)
Methanol	1.11	36.92	-140.51	1.99
Propane	1.08	34.22	-138.65	1.23
Isooctane	1.13	26.32	-84.72	0.19
RMFD-303 <sup>b</sup>	1.13	27.58	-78.34	0.81

<sup>a</sup> Obtained by fitting the expression

$$S_{u0} = B_m + B_2(\phi - \phi_m)^2$$

to the data in Table 2 using the values  $\phi_m$  given Table 3B.  $\Delta$  is the standard deviation of a point from the fitted curve.

<sup>b</sup> Vapor above liquid at 298K.

TABLE 3B  
Parameters  $C_m$ ,  $C_2$ , and  $\phi_m^a$

	$T$ (K)	$\phi_m$	$C_m$ (cm/s)	$C_2$ (cm/s)	$\Delta$ (cm/s)
Methanol	298	1.11	43.70	-157.22	0.44
Propane	298	1.08	40.11	-186.48	0.28
Isooctane	298	1.13	33.72	-110.82	0.36
RMFD-303 <sup>b</sup>	298	1.13	35.58	-140.45	0.31
RMFD-303	350	1.11	41.92	-130.02	0.39

<sup>a</sup> Obtained by fitting the expression

$$S_u = C_m + C_2(\phi - \phi_m)^2$$

to the data in Fig. 5  $\Delta$  is the standard deviation of a point from the fitted curve.

<sup>b</sup> Vapor above liquid at 298K.

the resulting fits to the data are shown by the solid curves in Figs. 1-3. Also given in the table are the corresponding parameters for propane [16] and the standard deviations of the points from the fitted curves. It can be seen that overall fits to the power law and Arrhenius forms are about equally good; however, the parameters for the Arrhenius form vary erratically with equivalence ratio, making their physical significance somewhat obscure and smooth interpolation and extrapolation difficult. In addition the Arrhenius form is very sensitive to the adiabatic flame temperature  $T_f^0$ , which is in turn sensitive to the thermodynamic model used to calculate it. Thus the power

law relation Eq. (15) is considerably easier to use and is recommended for practical applications in the pressure range 1-50 atm and temperature range 350-700K, where  $\pm 10\%$  accuracy is sufficient. At room temperature the fit is not as good, and it is better to use the correlations given in the following section.

#### 4.2. Equivalence Ratio Dependence

The dependence of the burning velocity on the fuel-air equivalence ratio at the reference condition  $T_u = 298K$  and  $p = 1$  atm is shown in Fig. 5. Also included for comparison are data for propane

**TABLE 4**  
Parameters  $U$ ,  $E_A$ , and  $b^a$

Fuel	$\phi = 0.8$	$\phi = 1.0$	$\phi = 1.2$
$U$ (cm/s $\times 10^{-4}$ )			
Methanol	55.0	578	1.05
Propane	17.1	137	7.0
Isooctane	36.2	454	4.5
RMFD-303	10.9	52	2.9
$E_A$ (kcal/g mole)			
Methanol	77.2	105.9	45.7
Propane	72.5	95.6	66.9
Isooctane	79.7	107.5	63.8
RMFD-303	70.4	88.8	60.4
$b$			
Methanol	-0.25	-0.27	-0.10
Propane	-0.24	-0.29	-0.20
Isooctane	-0.25	-0.31	-0.15
RMFD-303	-0.19	-0.20	-0.12
$\Delta$ (cm/s)			
Methanol	2.81	3.37	3.87
Propane	2.79	2.75	2.18
Isooctane	2.03	3.01	2.23
RMFD-303	2.27	4.10	2.72

<sup>a</sup> Obtained by fitting the Arrhenius form

$$S_u = U(T_u^0(K)298)(p(\text{atm}))^b \exp(-E_A/R_f^0 T_f^0)$$

to the points in Figs. 1-3.  $\Delta$  is the standard deviation of a point from the fitted curve.

obtained from Ref. [16] and partially vaporized RMFD303 obtained from Fig. 6. Since direct measurements at  $T_u^0 = 298\text{K}$  cannot be made without cooling the bomb to temperatures below room temperature, the points in Fig. 5 are actually linear extrapolations of data in the range  $T_u^0 = 320\text{-}360\text{K}$ . For all fuels the burning velocity peaks at an equivalence ratio in the neighborhood of 1.1 and falls off for rich and lean mixtures. The points for methanol, propane, and isooctane in the range  $\phi = 0.8\text{-}1.4$  have been fit by second-degree polynomials of the form

$$S_u = C_m + C_2(\phi - \phi_m)^2. \tag{20}$$

The results are shown by the smooth curves in Fig. 5, and best-fit parameters  $C_m$ ,  $C_2$ , and  $\phi_m$  are

given in Table 3B. It can be seen that the parameters  $C_m$  are significantly greater than the corresponding parameters  $B_m$  obtained from the overall fit of Eq. (15) to the data in Figs. 1-3. This supports our previous observation that the power law form underestimates the burning velocities near room temperature for all fuels. This is also true of the Arrhenius form, and neither should be used below 350K except for making rough estimates.

The burning velocity for partially vaporized RMFD303-air mixtures at  $p = 1$  atm and  $T_u^0 = 298\text{K}$  are compared with those of fully vaporized RMFD303 at  $p = 1$  atm and  $T_u^0 = 350\text{K}$  in Fig. 6. The upper equivalence ratio scale is based on the measured vapor pressure of the fuel in the bomb and applies to both sets of data. The lower scale is based on the mass of fuel injected at 298K and applies only to the data at  $T_u^0 = 298\text{K}$ . At  $T_u^0 = 350\text{K}$  the measured fuel vapor pressures were within  $\pm 3\%$  of those calculated from the mass in-

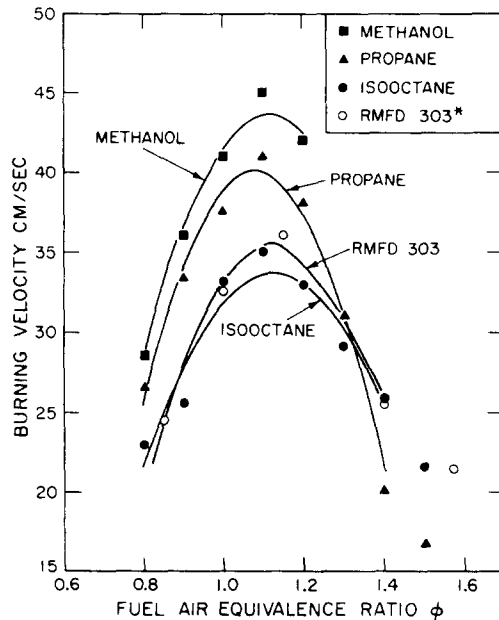


Fig. 5. Dependence of the burning velocity of mixtures of methanol, propane, isooctane, and partially vaporized RMFD303 with air on the fuel-air equivalence ratios determined from the vapor pressure of the fuel. The points for propane are from Ref. [16]. The points for RMFD303 correspond to those in Fig. 6. The curves are least squares fits of Eq. (20) to the points in the range  $\phi = 0.8\text{-}1.4$ .

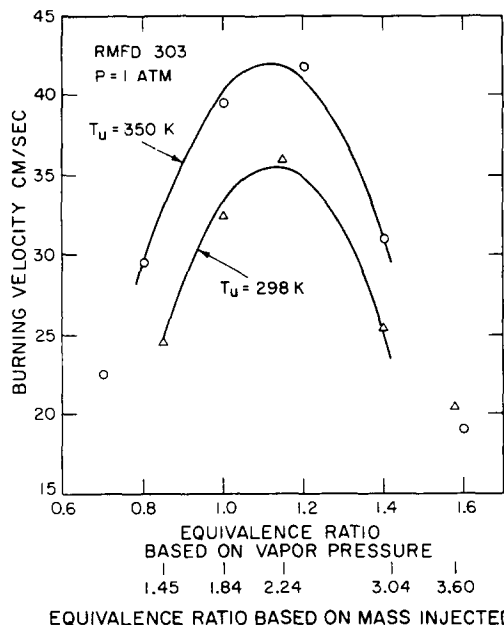


Fig. 6. Dependence of the burning velocity of RMFD303-air mixtures on fuel-air equivalence ratio  $\phi$  at  $p = 1$  atm and  $T_u^0 = 298$  and  $350$  K. At  $T_u^0 = 298$  K, RMFD303 does not completely vaporize and two equivalence ratio scales are shown: one based on vapor pressure and the second on mass of fuel injected.

jected using the ideal gas equations of state, indicating the fuel was fully vaporized. The smooth curves are fits to the polynomial form Eq. (20), for which the coefficients are given in Table 3B. Although the equivalence ratio based on vapor pressure and mass injected differ considerably at  $T_u^0 = 298$  K, there is no apparent effect on the burning velocity when the equivalence ratio is computed from the vapor pressure. This is consistent with the previous observation that the burning velocities of the fuels studied is relatively insensitive to fuel type, and thus the change in composition due to partial vaporization produces no measurable effect. This is of considerable interest in connection with the cold-starting problem in spark ignition engines.

#### 4.3. Effect of Inert Diluent

The effect of diluting stoichiometric isooctane-air mixtures with simulated combustion products was

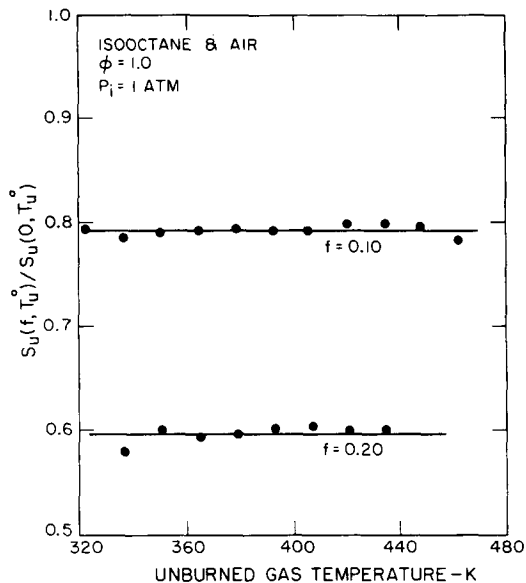


Fig. 7. Effect of diluting stoichiometric isooctane-air mixtures with simulated combustion products. The ratio of the burning velocities with and without dilution is shown as a function of unburned gas temperature at a total pressure of 1 atm for diluent mass fractions  $f = 0.1$  and  $0.2$ .

measured for an initial temperature  $T_1 = 298$  K and pressure  $p_1 = 1$  atm. A mixture of 15% carbon dioxide and 85% nitrogen by volume was used to simulate combustion products. This mixture has a molecular weight of 30.4 and a heat capacity which approximately matches that of the combustion products. The results are shown in Fig. 7, where the ratio of the burning velocities with and without dilution are plotted as a function of unburned gas temperature for diluent mass fractions  $f = 0.1$  and  $0.2$ . It can be seen that the decrease in burning velocity is independent of temperature and can be represented by the expression

$$S_u(f, T_u^0)/S_u(0, T_u^0) = 1 - 2.1f. \quad (21)$$

## 5. DISCUSSION

### 5.1. Methanol Air Mixtures

Laminar burning velocities for methanol-air mixtures at room temperature  $T_u^0 = 298$  K have been measured by Gibbs and Calcote [8] at  $p = 1.0$  atm

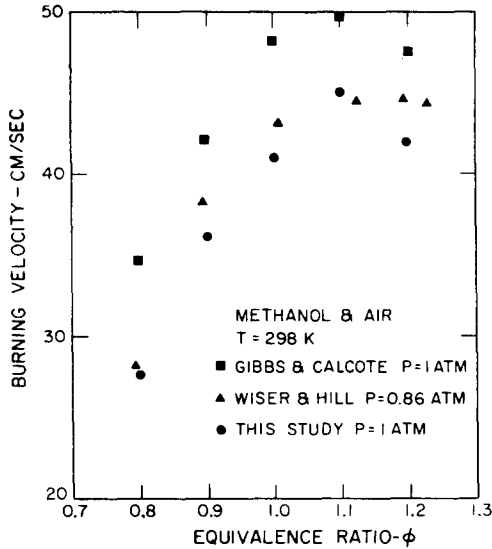


Fig. 8. Comparison of room temperature burning velocities for methanol-air mixtures measured by Gibbs and Calcote [8] at 1.0 atm and Wisser and Hill [26] at 0.85 atm with those measured in this study at 1.0 atm as a function of fuel-air equivalence ratio.

using a bunsen burner and by Wisser and Hill [26] at  $p = 0.85$  atm using a horizontal tube. Their results are compared with those obtained in this study in Fig. 8 for equivalence ratios  $\phi = 0.8-1.2$ . Measurements at higher equivalence ratios cannot be made for methanol at  $p = 1$  atm and  $T_u = 298$ K due to its low vapor pressure. Taking into account the weak negative pressure dependence of the burning velocities, it can be seen that the results of Wisser and Hill are in excellent agreement with those of this study. The results of Gibbs and Calcote are systematically higher, and this is typical of the comparison between burning velocities measured on bunsen burners and those measured using tubes or constant volume bombs [11, 13]. The most probable source of such a systematic discrepancy is the relatively complicated geometry of a bunsen burner flame and the associated correction necessary to account for the effects of curvature.

Burning velocities for stoichiometric methanol-air mixtures have also been measured at high pressures and temperatures by Ryan and Lestz [10] using the constant volume bomb method. Their measurements were made along a single isentrope starting at  $p_1 = 4.0$  atm and  $T_1 = 477$ K and fit by

a function of the form

$$S_u = b_1(p/p_0)^{b_2} \exp(-b_3/T_u^0). \quad (22)$$

Because  $T_u^0$  and  $p$  are correlated along an unburned gas isentrope, the parameters of  $b_2$  and  $b_3$  are not independent and the particular values found depend on the functional form used to fit the measurements. The value of the pressure exponent  $b_2 = -0.095$  determined by Ryan and Lestz is in reasonable agreement with the value  $\beta = -0.13$  found in this study. The corresponding values of  $b_1$  and  $b_3$  are 4680.9 cm/s and 2086.6K. The burning velocities computed from Eq. (22) using these constants are shown in Fig. 9 as a function of unburned gas temperature at a pressure of 6 atm. Also shown are the corresponding values computed from Eq. (15) using the parameters in Table 2 found in this study. It can be seen that the burning velocities measured by Ryan and Lestz increase considerably faster with temperature than those measured in this study. The reasons for this are not clear but may be due to the difference in the procedures used to deduce the burning velocities from the pressure records. Ryan and Lestz used

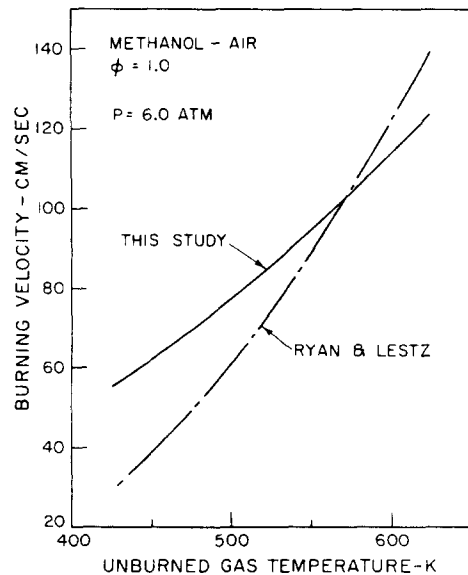


Fig. 9. Comparison of the burning velocities of stoichiometric methanol-air mixtures measured by Ryan and Lestz [10] and in this study at 6 atm as a function of unburned gas temperature.

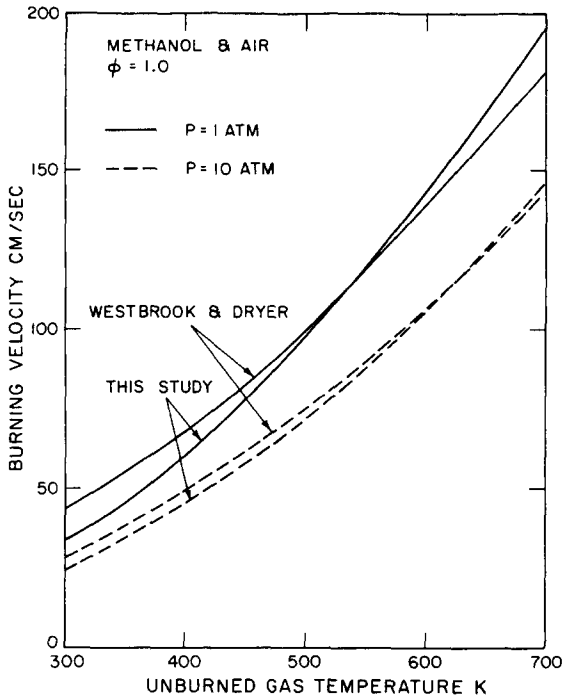


Fig. 10. Comparison of the burning velocities of stoichiometric methanol-air mixtures calculated by Westbrook and Dryer [7] with those measured in this study at 1 and 10 atm as a function of unburned gas temperature.

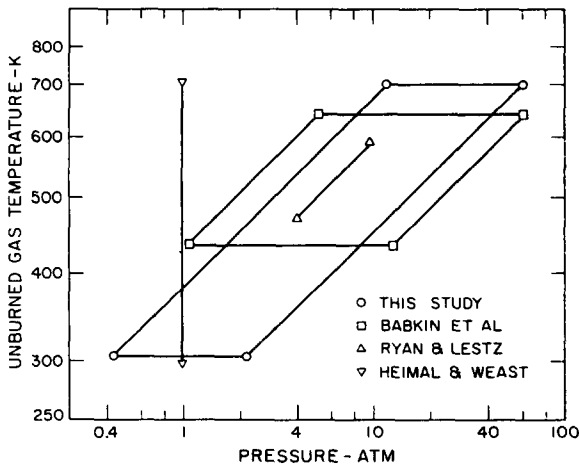


Fig. 11. Temperature and pressure ranges for which burning velocities were measured by various investigators: ●, this study; □, Babkin et al. [18]; △, Ryan and Lestz [10]; ▽, Heimel and Weast [28].

stepwise numerical procedures, while analytic procedures were used in this study.

Laminar burning velocities of methanol-air mixtures have also been calculated by Westbrook and Dryer [7] using a detailed chemical kinetic model. Figure 10 shows a comparison between the predicted burning velocities and those measured in this study for pressures of 1 and 10 atm. It can be seen that the agreement is remarkably good, although the temperature dependence of the measured velocities is slightly stronger than that predicted.

## 5.2. Isooctane-Air-Diluent Mixtures

Measurements of the burning velocity of isooctane-air mixtures have been made as a function of temperature at atmospheric pressure by Dugger and Graab [17], Heimel and Weast [28], and Gibbs and Calcote [18] using bunsen burners and at high pressures by Babkin et al. [18] and Ryan and Lestz [10] using constant volume bombs similar to that employed in this study. The ranges of temperatures and pressures over which the measurements were made are shown in Fig. 11, and the results are compared in Fig. 12 at pressures of 1, 6, and 40 atm. The points show individual measurements and the coded curves show smoothed fits to the data made using various assumed functional forms. The results of this study are given by

$$S_u = 27p^{-0.16}(T_u^0/298)^{2.18}, \quad (23)$$

Babkin et al. give

$$S_u = (404 \log T_u^0 - 1008)p^{-(0.39 - 0.0004T_u^0)}, \quad (24)$$

Ryan and Lestz give

$$S_u = 2965.5p^{-0.051}e^{-(2008.8/T_u^0)}, \quad (25)$$

and Heimel and Weast give

$$S_u = 12.1 + 21.9(T_u^0/298)^{2.19} \quad (26)$$

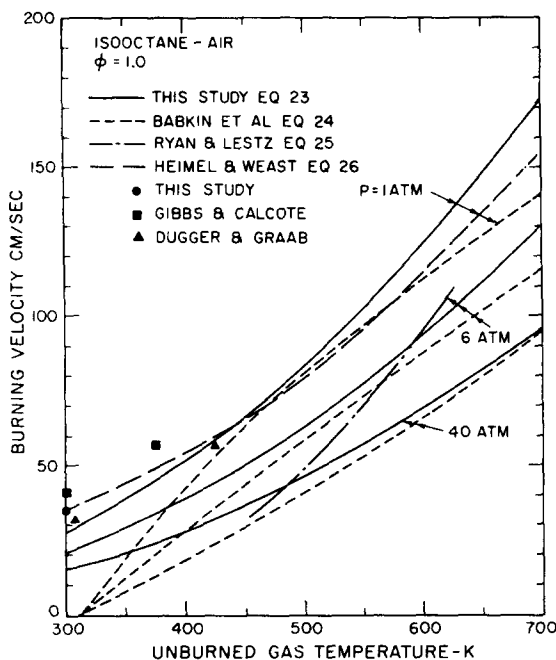


Fig. 12. Comparison of burning velocities of stoichiometric isooctane-air mixtures measured by various investigators at 1, 6, and 40 atm as a function of unburned gas temperature. Points are experimental measurements. Curves were computed from the equations indicated. See text for references.

at 1 atm. In the above equations,  $S_u$  is in cm/s,  $p$  is in atm, and  $T_u^0$  is in degrees K. In the range where the data actually overlap the results of this study agree well with those of Babkin et al., Heimal and Weast, and Dugger and Graab. The results of Gibbs and Calcote are somewhat high, and those of Ryan and Lestz show a significantly stronger temperature dependence. This is similar to the situation for methanol-air mixtures shown in Figs. 8 and 9 and is probably due to the same causes. It can also be seen from Eq. (24) and Fig. 12 that the functional form used by Babkin et al. to fit their results has an unrealistic zero at  $T_u^0 = 312\text{K}$  and cannot be used for extrapolation to low temperatures. Equation (23) used in this study is very much better in this respect, although, as previously noted, it underestimates the measured burning velocities at temperatures less than  $\sim 350\text{K}$ . This could be corrected by inclusion of an additive constant of the type included by Heimal and Weast in Eq. (26). Equation (23) also given slightly larger burning

velocities at high temperatures than those measured by Heimal and Weast; however, considering the long extrapolation in pressure required to obtain the values above  $600\text{K}$ , the agreement is well within experimental error.

The effect of diluting stoichiometric isooctane-air mixtures with simulated combustion products has been studied by Ryan and Lestz [10] at  $p = 6$  atm and  $T_u^0 = 520\text{K}$ . For diluent mass fractions up to  $f = 0.3$  they found

$$S_u(f)/S_u(0) = 1 - 2.5f, \quad (23)$$

in reasonably good agreement with Eq. (21).

### 5.3. RMFD303-Air Mixtures

No comparable measurements of burning velocities for wide-boiling-range blends such as RMFD303 have been reported. However, the fact that its burning velocity does not differ significantly from that of isooctane and depends only on the partial pressure of the vaporized fraction is consistent with the observations of Gibbs and Calcote [8], who found that for relatively heavy hydrocarbons, the burning velocities were roughly independent of both the number of carbon atoms and the molecular structure.

## 6. SUMMARY

Measurements of the burning velocity of practical fuel-air-diluent mixtures over a wide range of temperatures and pressures of interest for internal combustion engines and burners have been made. The fuels studied were methanol, isooctane, and indolene (RMFD303). The diluent used to simulate combustion products was 85%  $\text{N}_2$  and 15%  $\text{CO}_2$ . The measurements covered the range of fuel-air equivalence ratios  $\phi = 0.8-1.4$ , diluent mass fractions  $f = 0-0.2$ , pressures  $p = 0.4-50$  atm, and unburned gas temperatures  $T_u^0 = 300-700\text{K}$ . The results for  $p = 1$  and  $T_u^0 = 298\text{K}$  are given in Figs. 5 and 6. For temperatures above  $350\text{K}$ , the data for all fuels including propane which was studied previously [16] could be fit within  $\pm 10\%$  by the

simple power law

$$S_u = S_{u0}(T_u^0/T_0)^\alpha(p/p_0)^\beta(1 - 2.1f), \quad (24)$$

where

$$S_{u0} = B_m + B_2(\phi - \phi_m)^2,$$

$$\alpha = 2.18 - 0.8(\phi - 1),$$

$$\beta = -0.16 + 0.22(\phi - 1),$$

$$T_0 = 298\text{K},$$

$$p_0 = 1 \text{ atm},$$

and the constants  $B_m$ ,  $B_2$ , and  $\phi_m$  are given in Table 3A. Note that  $S_{u0}$  is a weakly decreasing function of increasing molecular weight, while within experimental error,  $\alpha$  and  $\beta$  are independent of fuel type. In regions of overlapping data, the results of this study generally agree well with those of previous studies.

#### APPENDIX: DISPLACEMENT VOLUME CORRECTIONS

For the unburned gas, the displacement volume correction can be expressed

$$a_u = a_w + a_f,$$

where  $a_w$  and  $a_f$  are the contributions from the wall boundary layer and the preheat layer ahead of the reaction front. For the burned gas, the correction can be expressed

$$a_b = a_d + a_e + a_r + a_g,$$

where  $a_d$ ,  $a_e$ ,  $a_r$ , and  $a_g$  are the contributions from the ignition energy input, the electrode boundary layer, radiation heat loss, and the burned gas temperature gradient.

#### Wall Boundary Layer

The boundary layer displacement thickness

$$\begin{aligned} \delta_w &= \int_0^\infty \left( \frac{\rho_u}{\rho_u^0} - 1 \right)_w dz \\ &= \frac{m_1}{A_c} \int_x^1 (v_u^0 - v_u)_w dx' \end{aligned} \quad (A1)$$

in a gas subject to a time-dependent pressure is given by [29]

$$\begin{aligned} \delta_w &= 2 \left( 1 - \frac{1}{\gamma_u} \right) \left( \frac{\nu_1 p_1}{\pi p} \right)^{1/2} \\ &\times \int_{p_1}^p \left( \int_{t'}^t \frac{p''}{p} dt'' \right)^{1/2} \left( \frac{p}{p'} \right)^{(2\gamma_u - 1)/\gamma_u} \\ &\times \frac{dp'}{p}, \end{aligned} \quad (A2)$$

where

$$\nu = \lambda/\rho c_p \quad (A3)$$

is the thermal diffusivity and  $\lambda$  is the thermal conductivity. In the derivation of Eq. (A2), it has been assumed that the thermal conductivity can be approximated by

$$\lambda = \lambda_0 T/T_0 \quad (A4)$$

and that for isentropic compression of an ideal gas

$$(T_u^0/T_1)^{\gamma_u/(\gamma_u - 1)} = (\rho_u^0/\rho_1)^{\gamma_u} = p/p_1. \quad (A5)$$

For rapidly increasing pressures such as those occurring in combustion bombs, Eq. (A2) can be integrated approximately to give

$$\begin{aligned} \delta_w &\approx \left( \frac{4\nu_1 \tau_f}{\pi} \right)^{1/2} \left( \frac{p_1}{p} \left( 1 - \frac{p_1}{p} \right) \right)^{1/2} \\ &\times \left( \left( \frac{p}{p_1} \right)^{(\gamma_u - 1)/\gamma_u} - 1 \right), \end{aligned} \quad (A6)$$

where

$$\tau = p/(dp/dt) = p(dx/dp)/(dx/dt) \quad (A7)$$

is the characteristic time for the pressure increase. Using the exact equation

$$dx/dt = (\rho_u^0/\rho_1)(S_u A_f/V_c) \quad (A8)$$

and the simple but accurate approximation

$$x \approx (p/p_1 - 1)/(p_2/p_1 - 1), \quad (A9)$$

where

$$p_2/p_1 = (\gamma_f(T_f^0 - T_u^0)/T_1) + 1, \quad (\text{A10})$$

Eq. (A7) may be evaluated to give

$$\tau \approx (V_c/S_u A_f)((p_2/p_1) - 1)^{-1}(p/p_1)^{(\gamma_u-1)/\gamma_u}. \quad (\text{A11})$$

Combining Eqs. (A1), (A6), and (A11) and using the further approximations

$$V_f/V_c = (1 - (p_1/p)^{1/\gamma_u})/(1 - (p_1/p_2)^{1/\gamma_u}) \quad (\text{A12})$$

and

$$S_u = S_{u0}(T_u^0/T_0)^2, \quad (\text{A13})$$

we obtain the wall displacement volume correction

$$\begin{aligned} a_w &= \int_x^1 (v_u^0 - v_u) dx'/v_1 \\ &= 3\delta_w/r_c \\ &\approx B_w \left( \frac{p_0 T_1}{p_1 T_0} \right)^{1/2} \left( \left( \frac{p}{p_1} \right)^{(\gamma_u-1)/\gamma_u} - 1 \right) \\ &\quad \times \left( \frac{p_1}{p} \right)^{(2\gamma_u-1)/2\gamma_u}, \end{aligned} \quad (\text{A14})$$

where

$$B_w = \left( \frac{12T_0}{\pi\gamma_f T_f^0} \right)^{1/2} \left( \frac{v_0}{S_{u0} r_c} \right)^{1/2} \sim 0.02.$$

### Preheat Layer

For a reaction zone of zero thickness the temperature distribution in the preheat layer is given by [30]

$$T_u - T_u^0 = (T_f^0 - T_u^0)e^{-\xi}, \quad (\text{A15})$$

where

$$\xi = \rho_u^0 c_{pu} S_u \int_0^z \lambda_u^{-1} dz. \quad (\text{A16})$$

Using Eqs. (A3), (A4), (A13), and (A16) and noting that

$$dx = \frac{\rho_u A_f}{m_1} dz = \frac{A_f \lambda_u^0}{m_1 c_{pu} S_u} d\xi, \quad (\text{A17})$$

we find

$$\begin{aligned} a_f &= \int_x^1 \left( 1 - \frac{T_u}{T_u^0} \right) \frac{dx'}{\rho_u v_1} \\ &\approx -B_f \left( \frac{p_0 T_0}{p_1 T_1} \right) \frac{A_f}{A_c} \left( \frac{p_1}{p} \right)^{(2\gamma_u-1)/\gamma_u}, \end{aligned} \quad (\text{A18})$$

where

$$B_f = \frac{3T_f^0}{T_0} \left( \frac{v_0}{S_{u0} r_c} \right) \sim 0.02.$$

### Ignition Energy Input

Assuming that the energy input from the spark all goes into the burned gas and that the associated pressure rise in the bomb is negligible, we find for constant specific heats

$$\begin{aligned} E_d &\approx m_1 \int_0^x c_{pb}(T_b - T_b^0) dx' \\ &= m_1 p \frac{c_{pb}}{R_b} \int_0^x (v_b - v_b^0) dx'. \end{aligned} \quad (\text{A19})$$

This gives

$$a_d = \int_0^x (v_u^0 - v_b) \frac{dx'}{v_1} \approx - \left( 1 - \frac{1}{\gamma_b} \right) \frac{E_d}{pV_c} \quad (\text{A20})$$

and since the maximum energy stored in the ignition system condenser was 1 J,

$$a_d < 0.001 p_0/p.$$

### Electrode Boundary Layer

For two radial electrodes of radius  $r_e$  we have

$$a_e = 2 \int_0^x (v_b^0 - v_b) \frac{dx'}{v_1} \\ = \frac{4r_e}{V_c} \int_0^{r_f} \int_0^\infty \left( \frac{v_b^0}{v_b} - 1 \right) dz dr. \quad (\text{A21})$$

Assuming as a first approximation that

$$\int_0^\infty \left( \frac{v_b^0}{v_b} - 1 \right) dz \approx \frac{1}{2} \left( \frac{T_f^0}{T_1} - 1 \right) \left( \frac{\nu_1 r_f}{S_u} \right)^{1/2} \quad (\text{A22})$$

and using Eqs. (A3)–(A5) and (A13), we obtain

$$a_e \approx B_e \frac{T_0}{T_1} \left( \frac{p_0}{p_1} \right)^{1/2} \left( \frac{V_f}{V_c} \right)^{1/2} \left( \frac{p_1}{p} \right)^{(\gamma_u - 1)/\gamma_u}, \quad (\text{A23})$$

where

$$B_e = \frac{r_e T_f^0}{r_c T_0} \left( \frac{\nu_0}{S_u r_c} \right)^{1/2} \sim 0.002.$$

### Radiation Heat Loss

The radiation heat loss from the burned gas can be estimated using the relation

$$a_r = \frac{R_b}{p\nu_1 c_{pb}} \int_0^x c_{pb}(T_b^0 - T_b) dx' \\ = \frac{(\gamma_b - 1)}{\gamma_b p V_c} \int_0^t \Gamma_r A_f dt', \quad (\text{A24})$$

where  $\Gamma_r$  is the radiation heat loss per unit area of the flame front. For an optically thin sphere [31],

$$\Gamma_r \approx (1 - w_r)^{1/2} \epsilon_b \sigma T_b^4, \quad (\text{A25})$$

where  $\sigma = 5.67 \times 10^{-8} \text{ w/m}^2 \text{ K}^4$  is the Stefan-Boltzmann constant,  $w_r$  is the reflection coef-

ficient of the bomb wall,

$$\epsilon_b = (400/T_b) \left( (4/3) r_c (\chi_{\text{H}_2\text{O}} + \chi_{\text{CO}_2}) p/p_0 \right)^{1/2} \quad (\text{A26})$$

is the burned gas emissivity, and  $\chi$  denotes the mole fraction of the species indicated by the subscript. Using Eqs. (A5), (A8), (A9), (A13), (A25), and (A26), Eq. (24) can be evaluated approximately to give

$$a_r \approx B_r \frac{T_0}{T_1} \left( \frac{p_0}{p_1} \right)^{1/2} \frac{p_1}{p} \left( \left( \frac{p}{p_1} \right)^{(2 - \gamma_u)/2 \gamma_u} - 1 \right), \quad (\text{A27})$$

where

$$B_r = \frac{4(\gamma_b - 1)}{(2 - \gamma_u)} \left( (1 - w_r)(\chi_{\text{H}_2\text{O}} + \chi_{\text{CO}_2}) \frac{r_c}{3} \right)^{1/2} \\ \times \frac{400\sigma T_0 (T_f^0)^2}{p_0 S_{u0}} \sim 0.02.$$

### Burned Gas Temperature Gradient

Assuming constant specific heats, the correction for heat conduction from burned to unburned gas can be written

$$a_g = \frac{R_b}{p\nu_1 c_{pb}} \int_0^x c_{pb}(T_b^0 - T_b) dx' \quad (\text{A28}) \\ = \frac{(\gamma_b - 1)}{\gamma_b p V_c} \int_0^t \Gamma_g A_f dt',$$

where

$$\Gamma_g \approx \lambda_b \left( \frac{\partial}{\partial p'} T_b^0(p', p) \right)_f \left( \frac{\rho_f^0}{\rho_u^0} \right) \frac{dp}{dr_f} \quad (\text{A29})$$

is the heat flux per unit area from burned to unburned gas. Using the relations

$$T_b^0(p', p) = T_f^0(p')(p/p')^{(\gamma_b - 1)/\gamma_b} \quad (\text{A30})$$

and Eqs. (A3)–(A5), (A8), (A9), (A12), and (A13), we obtain

$$a_g \approx B_g \left( \frac{p_0}{p_1} \right) \frac{A_t}{A_c} \left( \frac{p_1}{p} \right)^{(\gamma_u - 1)/\gamma_u}, \quad (\text{A31})$$

where

$$B_g = \frac{3(\gamma_b - 1)}{\gamma_b(2 - \gamma_u)} \left( \frac{\nu_0}{S_{u0} r_c} \right) \sim 0.0003.$$

**NOMENCLATURE**

**Roman**

$a$	displacement volume correction
$A$	area
$c$	specific heat
$E$	energy
$f$	residual mass fraction
$g$	gravitational acceleration (9.806 m/s <sup>2</sup> )
$m$	mass
$p$	pressure
$r$	radius
$R$	specific gas constant
$S$	burning velocity
$T$	temperature
$v$	specific volume
$V$	volume
$w_r$	wall reflection coefficient
$x$	mass fraction
$z$	normal coordinate

**Greek**

$\alpha$	temperature exponent
$\beta$	pressure exponent
$\gamma$	specific heat ratio
$\delta$	displacement thickness
$\epsilon$	burned gas emissivity
$\eta$	$(\partial \ln v / \partial \ln p)_s$
$\lambda$	thermal conductivity
$\nu$	thermal diffusivity
$\xi$	Peclet number
$\pi$	3.1416
$\rho$	density
$\rho_{ah}$	density of species $a$ at top of bomb

$\rho_{a1}$	density of species $a$ at bottom of bomb
$\sigma$	Stefan-Boltzmann constant ( $5.67 \times 10^{-8}$ w/m <sup>2</sup> K <sup>4</sup> )
$\tau$	characteristic pressure rise time
$\phi$	fuel-air equivalence ratio
$\chi$	mole fraction

**Subscripts**

1	initial conditions
2	final condition
b	burned gas
c	combustion bomb
d	spark discharge
e	electrode
f	reaction front
g	burned gas temperature gradient
i	reference isentrope
$\eta$	correction for $\eta$ variation
0	reference condition: $p_0 = 1$ atm, $T_0 = 298$ K
p	constant pressure
r	radiation
s	constant entropy
T	constant temperature
u	unburned gas
v	constant volume
w	wall

**Superscripts**

0	adiabatic conditions
' , "	dummy variables

**Fitted Parameters**

$S_{u0}, \alpha, \beta$	Table 2
$U, E_A, b$	Table 4
$B_m, B_2, \phi_m$	Table 3A
$C_m, C_2, \phi_m$	Table 3B
$b_1, b_2, b_3$	Ryan and Lestz [10]

*The authors would like to thank Professor William Unkel and Mr. Bob Dezmelyk for their assistance in the design and installation of the A/D data acquisition systems used in these experiments and Mr. Fee Yee for his assistance with the con-*

struction of much of the instrumentation. They would also like to thank the Army Research Office and the National Science Foundation for their joint support of this work under grants DAAG29-78-C-0010 and ENG77-1466.

## REFERENCES

- Blizard, N. S., and Keck, J. C., SAE Paper 740191 (1974).
- Tabaczynski, R. J., Trinker, F. H., and Shannan, B. A. S., *Combust. Flame* 39:111 (1980).
- Libby, P. A., and Bray, K. N. C., *Combust. Flame* 39:33 (1980).
- Ferguson, C. R., and Keck, J. C., *Combust. Flame* 28:197 (1977).
- Ferguson, C. R., and Keck, J. C., *Combust. Flame* 34:85 (1979).
- Smoot, L. D., Hecker, W. C., and Williams, G. A., *Combust. Flame* 26:323 (1976).
- Westbrook, C., and Dryer, F., *Combust. Flame* 37:171 (1980).
- Gibbs, C. J., and Calcote, H. C., *Journal of Chemical Engineering Data* 4:226-237 (1959).
- Andrews, G. E., and Bradley, D., *Combust. Flame* 18:133 (1972).
- Ryan, T. W., and Lestz, S. S., *Automotive Engineering Congress*, Paper 800103, Detroit (1980).
- Garforth, A. M., and Rallis, C. J., *Combust. Flame* 19:275 (1972).
- Halstead, M. P., Pye, D. B., and Quinn, C. P., *Combust. Flame* 22:89 (1974).
- Andrews, G. E., and Bradley, D., *Combust. Flame* 19:275 (1972).
- Babkin, V. S., and Kozachenko, L. S., *Combustion, Explosion and Shock Waves* 2:46 (1966).
- Agnew, J. T., and Graiff, L. B., *Combust. Flame* 5:209 (1961).
- Metghalchi, M., and Keck, J. C., *Combust. Flame* 38:143 (1980).
- Nair, M. R. S., and Gupta, M. C., *Combust. Flame* 22:219 (1974).
- Babkin, V. S., V'yun, A. V., and Kozachinko, L. S., *Combustion, Explosion and Shock Waves* 3:221 (1967).
- Rallis, J. C., Garforth, A. M., and Steinz, J. A., *Combust. Flame* 9:345 (1965).
- Martin, M. K., and Heywood, J. C., *Combustion Science and Technology* 15:1 (1977).
- JANAF Thermochemical Tables*, Dow Chemical Company, Clearinghouse, Springfield, VA.
- Rossini, F. D., Pitzer, K. S., Arnett, R. L., Bramm, R. M., and Pimentel, G. C., *Selected Values of Physical and Thermodynamic Properties of Hydrocarbons and Related Compounds*, Carnegit Press, Pittsburgh, 1953.
- Groff, E. G., *Central States Meeting of the Combustion Institute*, Warren, Michigan, Paper CSS/CI 81-14, March 1981.
- Lavoie, G. A., *Sae Congress and Exposition*, Detroit, February 1978, Paper 780229.
- Semenov, N. N., N.A.C.A. TM1026, September 1942.
- Wiser, W. H., and Hill, G. R., *Fifth Symposium (International) on Combustion*, 1955, p. 553.
- Dugger, G. L., and Graab, D. D., *Fourth Symposium (International) on Combustion*, 1952, p. 302.
- Hiemel, S., and Weast, R. C., *Sixth Symposium (International) on Combustion*, 1957, p. 37.
- Keck, J. C., *Letters in Heat and Mass Transfer* 8:313 (1981).
- Spalding, D. B., *Combust. Flame* 1:296 (1957).
- Hottel, H. C., and Sarofim, A. F., *Radiative Heat Transfer*, McGraw-Hill, New York, 1967.

Received 15 September 1981; revised 12 February 1982